JOURNAL OF APPLIED ELECTROCHEMISTRY 18 (1988) 831–838

A.c. corrosion of nickel in sulphate solutions

T. C. TAN, D-T. CHIN*

Department of Chemical Engineering, National University of Singapore, Kent Ridge, Singapore 0511

Received 18 February 1988

The corrosion of nickel under the influence of alternating current (a.c.) in pH 1–7 Na_2SO_4 solutions has been investigated with an alternating voltage (a.v.) modulation technique. The anodic polarization curves and pitting behaviour of nickel were examined with the superimposition of sinusoidal, square, and triangular a.v. over a range of a.v. magnitudes of 0–5000 mV r.m.s., and a.v. frequencies of 20–5000 Hz. It was found that a.v. reduced the passive d.c. potential regime by increasing the critical current density prior to passivation and by shifting the active–passive transitional potential toward the positive direction. In acidic sulphate solutions, a.v. increased the current density in the passive regime in a way similar to the addition of chloride ions. A.v. destroyed the passivity and enhanced the pitting corrosion of nickel at both the passive and transpassive d.c. potentials. The passivity of nickel was destroyed regardless of the a.v. waveforms. Triangular a.v. caused the severest destruction of passivity; this was followed by sinusoidal and square wave a.v.

1. Introduction

Alternating current (a.c.) is used in the electroplating industry to improve the corrosion of nickel anodes in nickel plating baths [1]. A.c. behaves as a depolarizer. It reduces the protective passive film of nickel during the negative half-cycles, and causes the unprotected nickel to dissolve during the positive half-cycles. The current efficiency and rate of nickel dissolution increase with increasing magnitude of a.c.

Early investigations of the effect of 50–60 Hz sinusoidal a.c. on nickel corrosion were made by Feller [2], Devay *et al.* [3], Abd El Rehim and Abd El Halim [4], and Deo *et al.* [5]. These investigations were conducted by superimposing a.c. onto either: (i) a galvanostatic d.c. circuit [4–5]; or (ii) a potentiostatic d.c. circuit [2–3]. The galvanostatic method had the drawback that it did not permit the examination of passivity phenomena. The second method requires complex electronic instrumentation [6] to simultaneously control the galvanostatic a.c. current and the potentiostatic d.c. potential. The method also suffered from a stability problem because of incomplete filtration of a.c. in the d.c. potential control circuit [7].

Recently, Chin and coworkers [8] have developed an alternating voltage (a.v.) modulation technique for studying the mechanism of a.c. corrosion. In this method, an alternating voltage signal, instead of an alternating current, was superimposed onto a d.c. potential by connecting an a.v. signal generator to d.c. potentiostat. The resulting composite potential consisting of a.v. and d.c. potential was applied between the working and reference electrodes in the corrosion environment. The electric circuit was constructed so as to enable measurement of the time-averaged d.c. current as a function of d.c. potentials using a d.c. potential sweeping circuit. This method had the advantage that the measurement was potentiostatically controlled, and the effect of a.v. on the active, passive, and transpassive states of the corrosion system could be analyzed from the experimental data. The a.v. modulation technique has been used in the investigation of a.c. corrosion of iron [9–10], zinc [11], copper [12], stainless steels [13–14], and aluminum [15–16] in various aqueous environments.

In the present investigation, the a.c. corrosion of nickel in acidic and neutral sulphate solutions is examined with the a.v. modulation technique. The polarization measurements are made to determine the effect of a.v. magnitude, a.v. waveform, and a.v. frequency on the passivity of nickel in the solutions. The pitting behaviour of nickel under the influence of a.v. is examined with the potentiostatic pitting test and optical photomicroscopy. The results are compared to the pitting corrosion of nickel caused by the addition of chloride ions.

2. Experimental details

The electric circuit for a.v. modulation and the experimental set-up have been described in previous publications [8–16], and will not be repeated here. The solution used in the present study was 1 N Na_2SO_4 (pH 1–7), which was prepared by dissolving Merck analytical grade chemicals in deionized water and was adjusted to the desired pH value by addition of small amount of H_2SO_4 or NaOH. The solution was deaerated by bubbling nitrogen gas before and during the experiments. A stationary circular nickel† disc having an exposed area of 0.307 cm^2 was used as the

* *Present address*: Department of Chemical Engineering, Clarkson University, Potsdam, New York 13676, USA. To whom correspondence should be addressed.

† Composition of nickel (wt%): Cu 0.01, Si 0.02, Mn 0.23, Fe 0.01, S 0.003, C 0.06, Ni 99.67.

0021-891X/88 $03.00 + .12

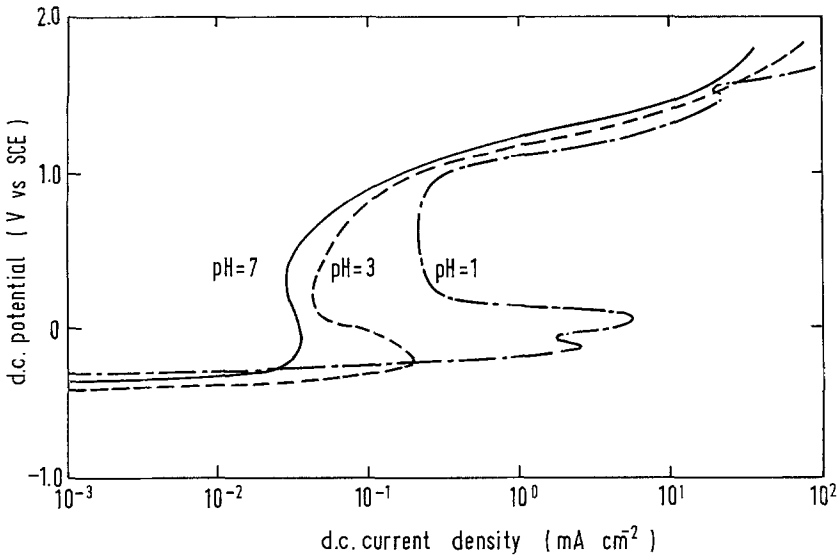

Fig. 1. Anodic polarization curves of nickel in 1 N sodium sulphate solutions at pH 1–7, 27° C. Scan rate = 50 mV min^{-1}.

working electrode. A 1 l Plexiglas cell equipped with a platinum counter electrode and a saturated calomel reference electrode (SCE) were used for the experiments. For each run the working electrode was polished to 600 grit smoothness, degreased in alcohol, and cleaned in concentrated sulphuric acid. It was then introduced into the cell and was cathodically activated in the test electrolyte at −3.0 V vs SCE for 3 min. The cathodic and anodic polarization curves with superimposed a.v. were measured with the previously described a.v. modulation circuit and d.c. potential sweep procedures [16] at a d.c. potential scan rate of 50 mV min^{-1}. The measurements were made for three different a.v. waveforms (sinusoidal, square and triangular waves) over a range of a.v. magnitude from 0 to 5000 mV r.m.s. (root mean square), and a.v. frequencies from 20 to 5000 Hz. All the measurements were made at a constant room temperature of 27 ± 1° C.

Potentiostatic pitting tests of nickel samples having 1.287 cm^2 exposed area were made at selected d.c. potentials with the a.v. modulation technique. A run was terminated after 5 C of d.c. had been passed through the cell. Pitting damages of the nickel sample were examined with an optical microscope.

3. Results and discussion

3.1. *D.c. polarization curves without a.v.*

To establish a basis for comparing with a.v. modulation, a particular set of runs was made to determine the anodic polarization curves of nickel in sodium sulphate solutions without any superimposed a.v. The results are given in Fig. 1 for a range of pH 1–7. In pH 1–3 Na_2SO_4 solutions, the anodic polarization curves of nickel exhibited distinct active, passive and transpassive states, with the active–passive transition occurring at 0.1 V vs SCE and the passive–transpassive transition occurring at 1.0 V vs SCE. Increasing pH decreased the peak critical current density prior to the transition to passivity as well as the passivity current density in the passive regime. The polarization curve for the pH 7 solution showed the spontaneous passivation of nickel upon polarization at the anodic potentials. The passive–transpassive transitional potential and the corrosion potential (or rest potential) were not changed by increasing pH values.

3.2. *Effect of a.v. on nickel polarization in acidic sulphate solutions*

Figure 2 shows the effect of 60 Hz sinusoidal a.v. on the anodic polarization of nickel in pH 1 Na_2SO_4 solution. In the acidic sulphate solution, a.v. increased the current density in the active regime, and progressively shifted the active–passive transitional potential toward the positive direction. The critical current density at the active–passive transitional potential increased with increasing magnitude of a.v. In the passive regime, a.v. increased the passivity current density and diminished the span of passive potentials. At the a.v. magnitudes greater than 1500 mV r.m.s., the passive regime was completely eliminated, and the polarization curves exhibited a direct transition from the active to the transpassive states as shown in Fig. 2. The behaviour was similar to the a.v. modulation of iron in perchlorate solutions [10].

To explain the observed phenomena, one should note that there are four processes occurring during the anodic polarization of nickel in acidic sulphate solutions. These are: (i) active anodic dissolution of nickel; (ii) formation of protective nickel oxide films at the passive d.c. potentials; (iii) oxygen evolution reaction on the oxide film at transpassive d.c. potentials; and (iv) breakdown of oxide film and transpassive dissolution of nickel at the film-damaged locations. Without any superimposed a.v. the four processes took place at three distinct d.c. potential regimes during the potential sweep, with process (i) occurring at the active regime; process (ii) at the passive regime; and processes (iii) and (iv) at the transpassive potential regime. With superimposed a.v., the four processes could take place simultaneously at a given d.c. potential because of the periodic fluctuations of instantaneous potentials between a high and a low value.

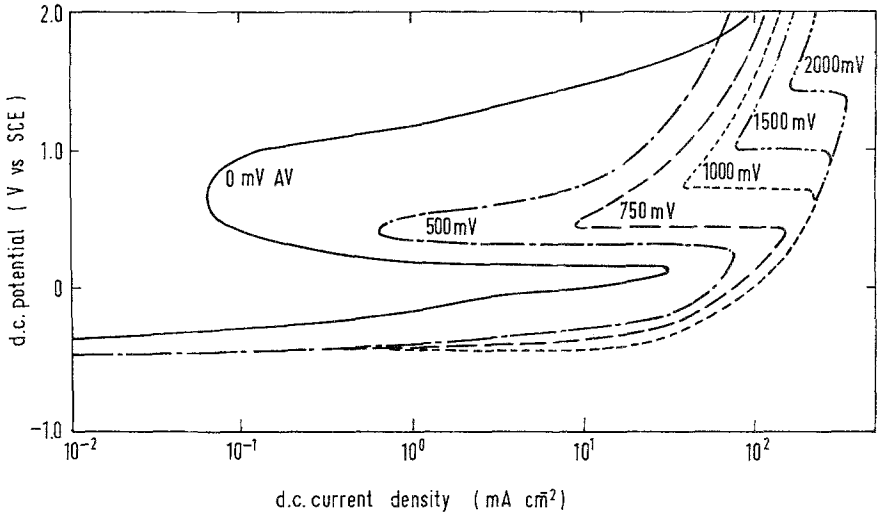

Fig. 2. Effect of 60 Hz sinusoidal a.v. on the anodic polarization curves of nickel in pH 1 sodium sulphate solution.

The present polarization curves suggest that at sufficiently positive d.c. potentials, a.v. selectively destroyed the protective oxide film of nickel at its weak locations, where the unprotected nickel dissolved at a high rate to form localized pits on the nickel surface. On the areas where the oxide film remained intact, oxygen evolution reaction took place during the positive half-cycles of a.v. This combined oxygen evolution reaction at the oxide covered areas and nickel dissolution at the oxide removed areas caused the passive–transpassive transitional potential to shift toward the positive direction and the current density in the passive regime to increase with increasing a.v. values.

Figure 3 shows the effect of sinusoidal a.v. frequency on the anodic d.c. polarization curves of nickel in pH 1 sodium sulphate solutions. The curves are given for a range of a.v. frequencies from 20 to 5000 Hz, while the a.v. magnitude was kept at a constant value of 750 mV r.m.s. There was no significant change on the shape of d.c. polarization curves at the low frequency range of 20–200 Hz. At higher frequencies, a portion of the a.c. passing across the electrode–electrolyte interface became non-faradaic, and was consumed in the charge and discharge of the electric double layer at the electrode surface. Thus, the effect of a.v. decreased with increasing frequency as shown in the figure.

In the acidic sulphate solutions, a.v. slightly shifted the corrosion potential of nickel toward the negative direction. However, the extent of the corrosion potential shifts was not a strong function of a.v. magnitude and a.v. frequency as noted in Figs 2 and 3.

3.3. *Effect of a.v. on nickel polarization in neutral sulphate solutions*

The effect of 60 Hz sinusoidal a.v. on the polarization of nickel in pH 7 Na_2SO_4 is shown in Fig. 4. The polarization curve without a.v. had no active dissolution regime, and nickel was spontaneously passivated upon the anodic polarization in the neutral sulphate solution. On the other hand, the polarization curves with superimposed a.v. exhibited distinct active, passive, and transpassive d.c. potential regimes. The alternating voltage shifted the active–passive transitional potential toward the positive direction. The peak critical current density prior to the

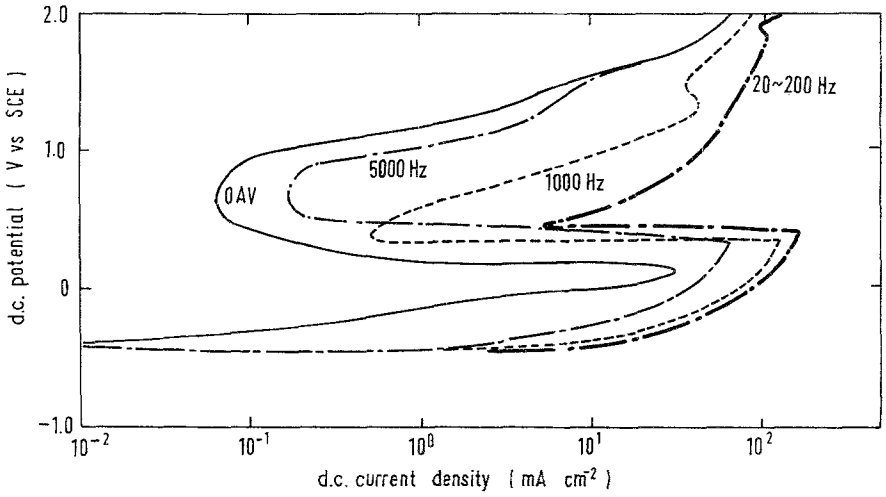

Fig. 3. Effect of a.v. frequencies on the anodic polarization of nickel in pH 1 sodium sulphate solution. The sinusoidal a.v. was maintained at a constant magnitude of 750 mV r.m.s.

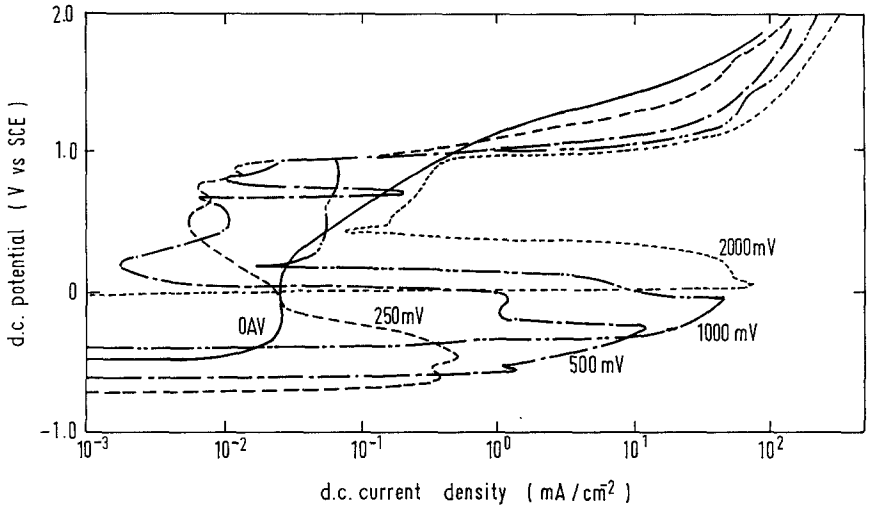

Fig. 4. Effect of 60 Hz sinusoidal a.v. on the anodic polarization curves of nickel in pH 7 sodium sulphate solution.

occurrence of passivation as well as the current density in the passive potential regime increased with increasing a.v. magnitude. A.v. also increased the d.c. current density in the transpassive regime; however, the passive–transpassive transitional potential was not affected by the application of a.v.

These results suggest that a.v. had the ability to reduce the passive oxide film of nickel in neutral sulphate solutions, when the anodic d.c. potential was low and the instantaneous potential was in the cathodic regime during the negative half-cycles of a.v. During the positive half-cycles of a.v., the bare nickel surface proceeded with the active dissolution without the protection of the oxide film. As the d.c. potential was scanned toward more positive values, the rate of the film reduction process decreased, and some of the nickel surface became re-passivated by a film repairing process during the positive half-cycles of a.v. The rate of film repairing process increased with increasing d.c. potentials. Eventually the rate of film repairing process exceeded that of the film reduction process, and the nickel surface became passivated at the active–passive transition potential as shown by the a.v. modulated polarization curves in Fig. 4. It is interesting to note that the passivity current density with 250 and 500 mV r.m.s. a.v. was smaller than that without superimposed a.v. However, the passivity current with a.v. was not stable as evidenced by the current spike on the 500 mV r.m.s. a.v. curve at 0.75 V vs SCE.

Figure 4 also indicates that the corrosion potential (or rest potential) of nickel in the neutral sulphate solution was first shifted by a.v. toward the negative direction. As the a.v. magnitude became greater than 250 mV r.m.s., the corrosion potential was systematically shifted back toward the positive direction. The corrosion potential data for the superimposition of 60 Hz sinusoidal a.v. are plotted in Fig. 5 for a range of a.v. from 0 to 5000 mV r.m.s. The initial drop in the corrosion potential provided further evidence that the oxide film on the nickel surface was removed by superimposition of a.v. The data for the a.v. greater than 250 mV r.m.s. could be regarded as the corrosion potentials of bare nickel surface in the deaerated sodium sulphate solution at pH 7. Figure 5 also shows the corrosion potentials with 60 Hz triangular and square-wave a.v. Qualitatively, the three different a.v. waveforms had a similar effect on the anodic polarization of nickel in both the acidic and neutral sulphate solutions. However, for a given r.m.s. value, the triangular a.v. caused the severest destruction of passivity and largest shift in the corrosion potential. This was followed by the sinusoidal a.v. and then the square-wave a.v. according to the sequence

Triangular a.v. > Sinusoidal a.v. > Square a.v. (1)

The sequence was similar to the effect of a.v. waveforms on the a.c. corrosion of iron [10], stainless steels [13–14], and aluminum [16] in aqueous environments. The sequence was explained by Chin and Sachadev [10] on the basis of peak voltage of different a.v. waveforms. The triangular a.v. had the highest peak voltage (1.73 times r.m.s. value) and accounted for the severest destruction of passivity. The sinusoidal a.v. had the second

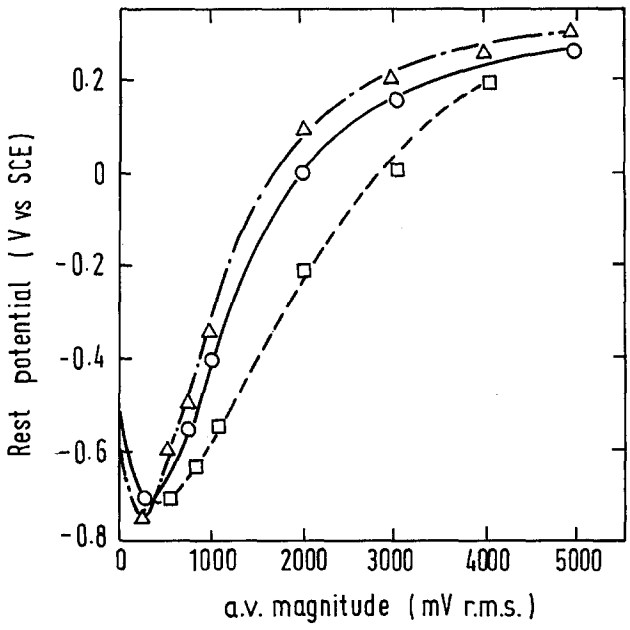

Fig. 5. Shift in the corrosion potential of nickel in pH 7 sodium sulphate solution by the superimposition of 60 Hz sinusoidal (○), square (□), and triangular (△) wave a.v.

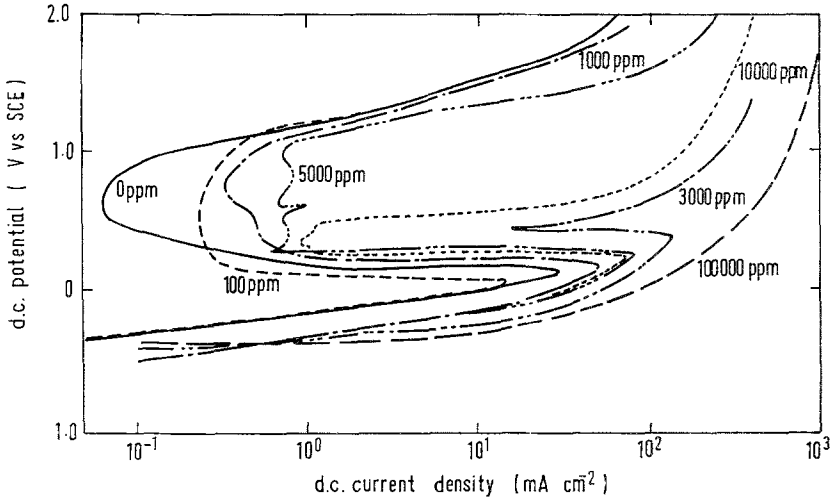

Fig. 6. Effect of the addition of NaCl on the anodic polarization curves of nickel in pH 1 sodium sulphate solution.

largest peak voltage (1.41 times r.m.s. value), and its effect on the nickel corrosion was between those of the triangular and square waves as shown in Fig. 5.

Experiments were also carried out to determine the effect of a.v. frequencies on the behavior of nickel in pH 7 Na_2SO_4 solutions. The results were similar to the nickel in acidic sulphate solutions that the a.v. affect diminished with increasing a.v. frequencies.

3.4. *Comparison with the addition of chloride ions*

The a.v. modulated polarization curves shown in Figs 2–4 had some features similar to the addition of chloride ions to aqueous environments. Chloride ion is known for its ability to chemically destroy the protective oxide film on metals and to cause localized attack on passivated surfaces. To compare the destruction of passivity by a.v. to that by chloride ions, a series of polarization measurements were made for nickel in 1 N Na_2SO_4 solutions containing various amounts of NaCl without any superimposed a.v. The results are given in Fig. 6 for pH 1 Na_2SO_4 solution containing 0–100 000 ppm NaCl and in Fig. 7 for pH 7 Na_2SO_4 solution containing 0–2500 ppm NaCl. In the acidic sulphate solutions, there was a remarkable similarity between the a.v. modulated polarization curves in Figs 2–3 and those with chloride ions shown in Fig. 6. Addition of chloride ions to the acidic sulphate solution caused the active–passive transitional potential to shift toward the positive direction, and the passive–transpassive transitional potential to shift toward the negative direction. As a consequence, the span of the passive potential regime was decreased by the addition of chloride ions. The critical current density at the active–passive transitional potential, and the current density in the passive regime increased with increasing concentrations of chloride ions. With the addition of 10^5 ppm NaCl, nickel no longer possessed a passive state as shown by the polarization curve in Fig. 6. This similarity between the polarization curves for a.v. modulation and those for the addition of chloride ions was also observed for iron and stainless steels in sulphate solutions [7, 14].

In pH 7 Na_2SO_4 solution, the destruction of passivity of nickel by chloride ions followed a pattern different from that of a.v. The chloride ion did not generate the active dissolution regime; instead, it shifted the passive–transpassive transitional potential toward the negative direction. With the addition of 2500 ppm NaCl, the passive–transpassive transitional potential was shifted from 1.0 V vs SCE to 0.5 V vs SCE as shown in Fig. 7.

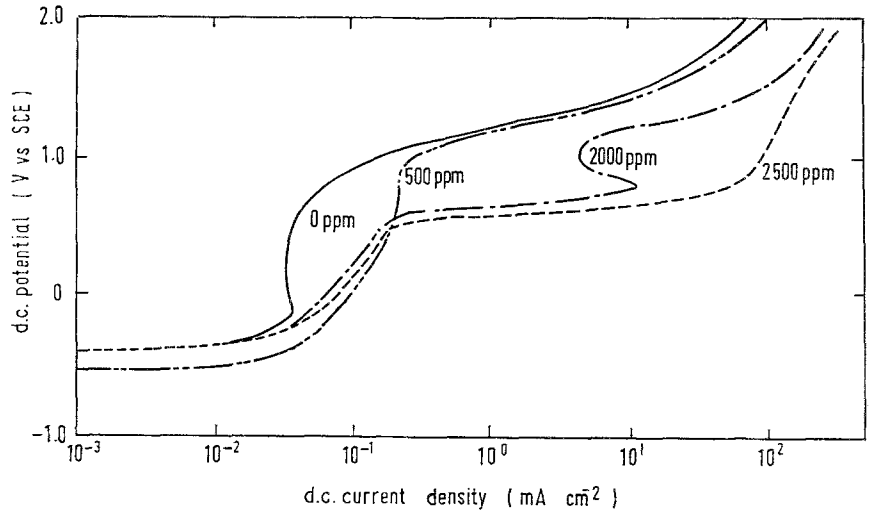

Fig. 7. Effect of the addition of NaCl on the anodic polarization curves of nickel in pH 7 sodium sulphate solution.

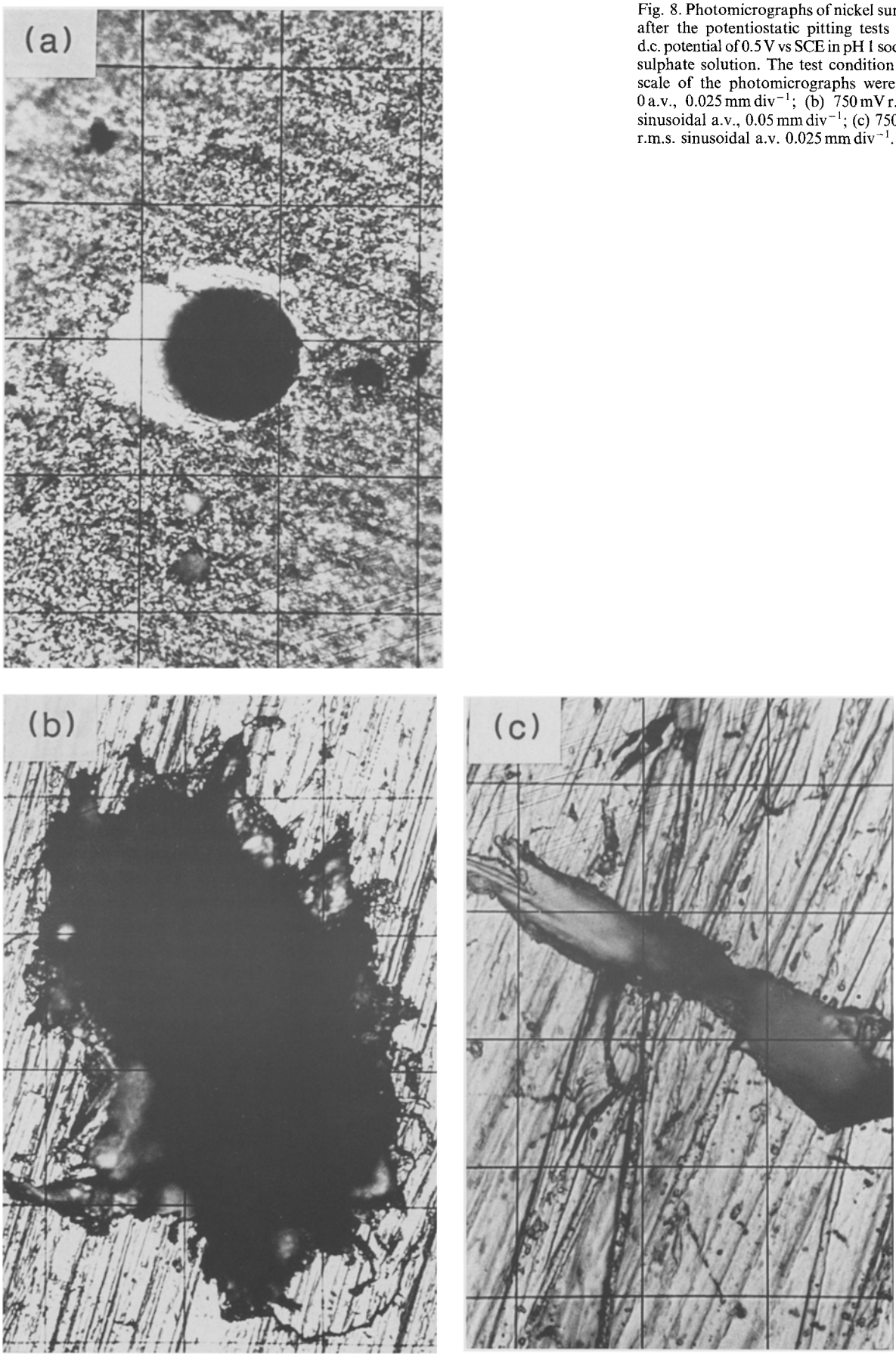

Fig. 8. Photomicrographs of nickel surface after the potentiostatic pitting tests at a d.c. potential of 0.5 V vs SCE in pH 1 sodium sulphate solution. The test condition and scale of the photomicrographs were: (a) 0 a.v., 0.025 mm div^{-1}; (b) 750 mV r.m.s. sinusoidal a.v., 0.05 mm div^{-1}; (c) 750 mV r.m.s. sinusoidal a.v. 0.025 mm div^{-1}.

3.5. *Results of potentiostatic pitting tests*

The photomicrographs of nickel specimens after the potentiostatic pitting tests in pH 1 and pH 7 Na_2SO_4 solutions are shown in Figs 8 and 9 (respectively). The photomicrographs were taken after 5 C of anodic d.c. current had been passed across the specimen with an exposed area of 1.287 cm^2. This amount of charge

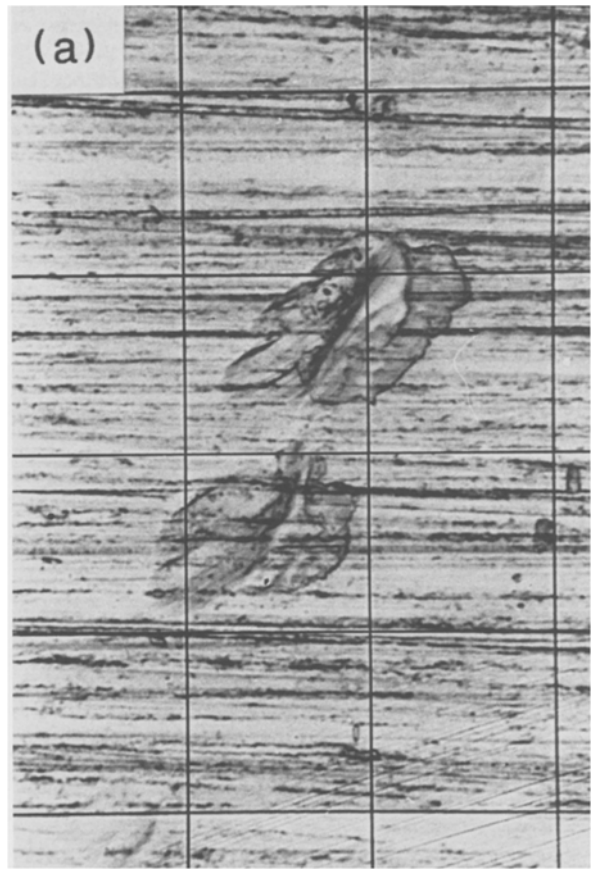

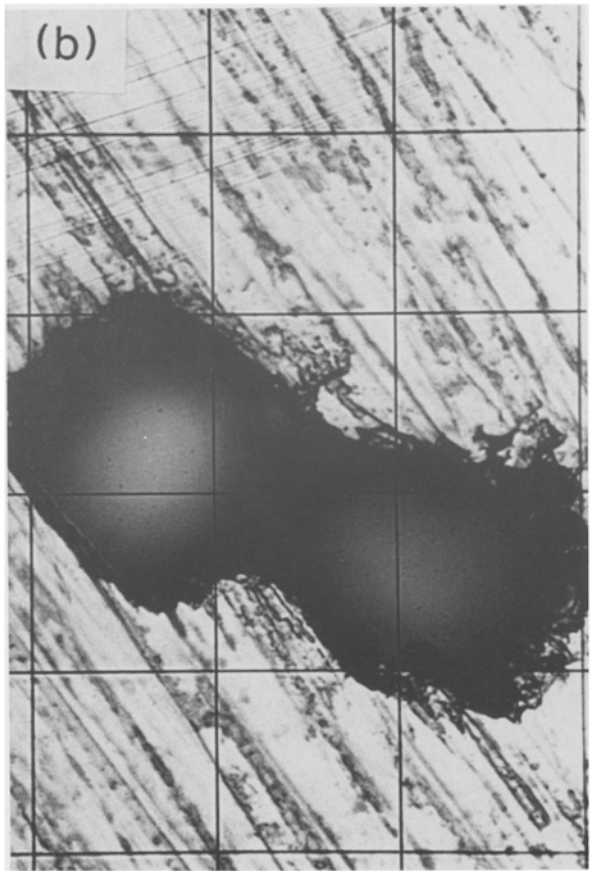

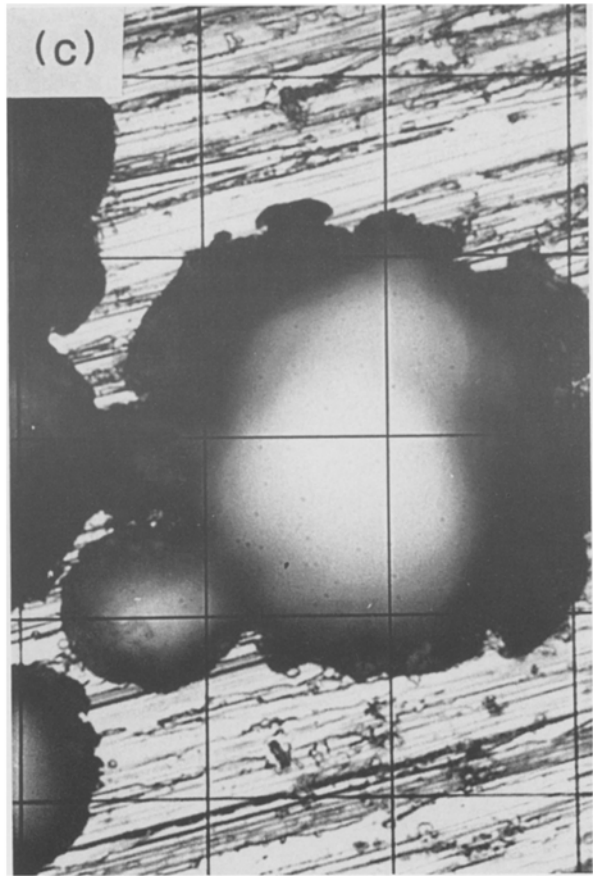

Fig. 9. Photomicrographs of nickel surface after the potentiostatic pitting tests at a d.c. potential of 0.75 V vs, SCE in pH 7 sodium sulphate solution. The test conditions were: (a) 0 a.v.; (b) 750 mV r.m.s. sinusoidal a.v. (c) 0 a.v. but with 2500 ppm NaCl. All the photomicrographs had a scale of 0.025 mm div^{-1}.

corresponded to a theoretical value of 1.5 mg of nickel removal or 0.001 mm of surface penetration if the nickel dissolution were taking place uniformly across the specimen surface.

The specimens in Fig. 8 were held at a passive d.c. potential of 0.5 V vs SCE in pH 1 sulphate solution. No a.v. was applied to the specimen in Fig. 8a, and 750 mV r.m.s. of 60 Hz sinusoidal a.v. was superimposed onto

the specimens in Figs 8b and 8c. Without any superimposed a.v. the specimen in Fig. 8a was covered by a layer of dark film, and had small isolated hemispherical pits of 0.003–0.03 mm in diameter, randomly scattered across the surface. The polishing lines resulting from the specimen preparation were no longer visible, suggesting that in addition to the pitting process, there was a mild uniform nickel dissolution process across the specimen surface in the acidic sulphate solution. With the application of a.v., the nickel dissolution process became more localized and the pitting process was enhanced as shown by the visible polishing lines and large pits in Figs 8b and 8c. The pits caused by a.v. did not have any particular shapes; they ranged from large irregular shaped pits in Fig. 8b to shallow elongated trenches in Fig. 8c. The pit shown in Fig. 8b was approximately 0.2 mm long by 0.13 mm wide and 0.04 mm deep.

Figure 9 shows the nickel specimens held at a passive d.c. potential of 0.75 V vs SCE in pH 7 Na_2SO_4 solutions. The specimen without any superimposed a.v. in the neutral sulphate solution was truly passivated and did not exhibit any dissolution as shown in Fig. 9a. With the application of 2000 mV r.m.s. of 60 Hz sinusoidal a.v., irregular shaped pits of approximately 0.05 mm in diameter and 0.03 mm deep were developed (Fig. 9b). Figure 9c shows the pits initiated by the addition of 2500 ppm NaCl to the pH 7 Na_2SO_4 solution; the specimen was held at the same d.c. potential of 0.75 V vs SCE without any superimposed a.v. Although the mechanism of destruction of passivity by chloride ions differed from that by a.v., they all removed the passivity on localized areas on nickel surfaces, resulting in a similar pitting process as shown in Figs 9b and 9c. The pitting behavior appeared to be predictable from the shapes of the d.c. polarization curves shown in Figs 2–4 and 6–7.

4. Conclusions

A study has been made of the effect of sinusoidal, square and triangular wave a.v. on the corrosion of nickel in pH 1–7 sodium sulphate solutions over a range of a.v. magnitudes from 0 to 5000 mV r.m.s., and a.v. frequencies from 20 to 5000 Hz. The results can be summarized as follows.

(1) The alternating voltage increased the nickel dissolution current density in both the active and transpassive d.c. potential regimes.

(2) The alternating voltage caused a shift in the corrosion potential in neutral sulphate solutions. The shift was toward the negative direction at low a.v. magnitudes. At a.v. magnitudes greater than 250 mV r.m.s., the corrosion potential was shifted back toward the positive direction. The corrosion potential in acidic sulphate solutions was not affected by the application of a.v.

(3) The alternating voltage increased the critical current density for passivity, and decreased the passive d.c. potential regime by shifting the active–passive transitional potential toward the positive direction. In acidic sulphate solutions, the passivity current density increased with increasing a.v. magnitudes; the effect was similar to that of the addition of chloride ions.

(4) A.v. destroyed the passivity of nickel and enhanced the pitting corrosion at both the passive and transpassive d.c. potentials.

(5) Triangular a.v. caused the severest destruction of passivity; this was followed by sinusoidal a.v. and then by square wave a.v.

(6) The effect of a.v. diminished with increasing a.v. frequencies.

Acknowledgement

This work was supported by a Research Grant from the National University of Singapore (NUS). The authors wish to acknowledge the assistance of Mr Ang Koon Chye in the experimental work. One of the authors, D-T. Chin, was a Visiting Professor at the NUS in 1987.

References

[1] S. Venkatesh and D-T. Chin, *Israel J. Chem.* **18** (1979) 56.
[2] H. G. Feller, 'Proc. 3rd Int. Congress Metallic Corrosion', Vol. II, Moscow (1969) pp. 555–562.
[3] J. Devay, B. Lengyel, S. S. Abd El Rehim, and J. Bakos, *Acta Chim. Acad. Sci. Hung.* **74** (1972) 193.
[4] S. S. Abd El Rehim and A. M. Abd El Halim, *ibid.* **80** (1974) 65.
[5] K. Deo, S. G. Mehendale, and S. Venkatachalam, *J. Appl. Electrochem.* **6** (1976) 37.
[6] R. L. Ruedisueli, H. E. Hager, and C. J. Sandwith, *Corrosion* **43** (1987) 331.
[7] D-T. Chin and T-W. Fu, *Corrosion* **35** (1979) 514.
[8] D-T. Chin, 'Proc. 4th Int. Congress Metallic Corrosion', Vol. 4, National Research Council of Canada, Ottawa (1984) pp. 96–103 (1984).
[9] D-T. Chin and S. Venkatesh, *J. Electrochem. Soc.* **126** (1979) 1908.
[10] D-T. Chin and P. Sachdev, *J. Electrochem. Soc.* **130** (1983) 1714.
[11] D-T. Chin, R. Sethi and J. McBreen, *ibid.* **129** (1982) 2677.
[12] R. Sethi and D-T. Chin, *J. Electroanal. chem.* **160** (1984) 79.
[13] J. L. Wendt and D-T. Chin, *Corros. Sci.* **25** (1985) 889.
[14] *Idem., ibid.* **25** (1985) 901.
[15] T. C. Tan and D-T. Chin, *J. Electrochem. Soc.* **132** (1985) 966.
[16] T. C. Tan and D-T. Chin, *Corros. Sci.*, submitted for publication.